



## RESEARCH PAPER

# Type-*f* thioredoxins have a role in the short-term activation of carbon metabolism and their loss affects growth under short-day conditions in *Arabidopsis thaliana*

Belén Naranjo<sup>1</sup>, Antonio Diaz-Espejo<sup>2</sup>, Marika Lindahl<sup>1</sup> and Francisco Javier Cejudo<sup>1,\*</sup>

<sup>1</sup> Instituto de Bioquímica Vegetal y Fotosíntesis, Universidad de Sevilla and CSIC, Avda Américo Vespucio, 49, 41092-Sevilla, Spain

<sup>2</sup> Instituto de Recursos Naturales y Agrobiología de Sevilla, CSIC, Avda Reina Mercedes, 10, 41012-Sevilla, Spain

\* Correspondence: [fcejudo@us.es](mailto:fcejudo@us.es)

Received 21 October 2015; Accepted 5 January 2016

Editor: Christine Raines, University of Essex

## Abstract

Redox regulation plays a central role in the adaptation of chloroplast metabolism to light. Extensive biochemical analyses *in vitro* have identified *f*-type thioredoxins (Trxs) as the most important catalysts for light-dependent reduction and activation of the enzymes of the Calvin–Benson cycle. However, the precise function of type *f* Trxs *in vivo* and their impact on plant growth are still poorly known. To address this issue we have generated an *Arabidopsis thaliana* double knock-out mutant, termed *trxf1f2*, devoid of both *f1* and *f2* Trxs. Despite the essential function previously proposed for *f*-type Trxs, the visible phenotype of the *trxf1f2* double mutant was virtually indistinguishable from the wild type when grown under a long-day photoperiod. However, the Trx *f*-deficient plants showed growth inhibition under a short-day photoperiod which was not rescued at high light intensity. The absence of *f*-type Trxs led to significantly lower photosynthetic electron transport rates and higher levels of non-photochemical energy quenching. Notably, the Trx *f* null mutant suffered from a shortage of photosystem I electron acceptors and delayed activation of carbon dioxide fixation following a dark–light transition. Two redox-regulated Calvin–Benson cycle enzymes, fructose 1,6-bisphosphatase (FBPase) and Rubisco activase, showed retarded and incomplete reduction in the double mutant upon illumination, compared with wild-type plants. These results show that the function of *f*-type Trxs in the rapid activation of carbon metabolism in response to light is not entirely compensated for by additional plastid redox systems, and suggest that these Trxs have an important role in the light adjustment of photosynthetic metabolism.

**Key words:** Carbon assimilation, chloroplast, fructose 1,6 bisphosphatase, photosynthesis, redox regulation, thioredoxin.

## Introduction

Chloroplasts are essential for plant life because these organelles perform photosynthesis, the process that allows the conversion of light energy into biomass with the concomitant production of molecular oxygen. In addition, chloroplasts act as sensors of environmental conditions, particularly light quantity and quality, thus playing an important role in harmonizing the growth of plant photosynthetic and non-photosynthetic tissues as well as the

adaptation of plants to the environment (Jarvis and López-Juez, 2013). To meet these requirements, chloroplast metabolism needs to respond rapidly to external and internal signals, redox regulation being an important aspect of this adaptability. Redox regulation is a post-translational modification consisting of the dithiol–disulphide interchange of selected and well-conserved cysteine residues of proteins. It is thus a reversible mechanism that allows the rapid

regulation of metabolic pathways (Buchanan *et al.*, 2012). Protein disulphide reductases such as thioredoxins (Trxs), small polypeptides of 12–14 kDa with a highly conserved active site (WCGPC) and a characteristic structure, the so-called Trx-fold, play a central role in redox regulation. Trxs catalyse the reduction of disulphide bridges in target proteins and, as a consequence, the two cysteine residues at the Trx active site become oxidized as a disulphide bridge. Therefore, for a new catalytic cycle this disulphide needs to be reduced, reducing power being provided by NADPH in a reaction catalysed by NADPH-dependent Trx reductase (NTR). This two-component redox system formed by NTR and Trx is universally distributed in all kinds of organisms from bacteria to fungi, animals, and plants (Jacquot *et al.*, 2009).

In contrast to heterotrophic organisms and non-photosynthetic plant tissues, redox regulation in chloroplasts has unique features. These organelles harbour a complex set of Trxs and Trx-like proteins (Lemaire *et al.*, 2007; Chibani *et al.*, 2009; Meyer *et al.*, 2012; Balsera *et al.*, 2014), which are not reduced by NADPH, but by ferredoxin (Fdx) reduced by photosynthetic electron transport in a process catalysed by a Fdx-dependent Trx reductase (FTR) found exclusively in plastids and cyanobacteria (Dai *et al.*, 2007). Therefore, chloroplast redox regulation is mediated by the Fdx/FTR/Trx system and, thus, is dependent on light. Initial biochemical analyses *in vitro* led to the identification of two types of Trxs in chloroplasts, termed *f* and *m*, based on their ability to reduce and activate fructose-1,6-bisphosphate phosphatase (FBPase) and NADP-malic dehydrogenase (NADP-MDH), respectively (Wolosiuk *et al.*, 1979). The availability of genome sequences from different plants has uncovered the complex set of chloroplastic Trxs, which in *Arabidopsis thaliana* include two isoforms of *f*-type, four isoforms of *m*-type, two isoforms of the *y*-type, and an *x*-type Trx (Lemaire *et al.*, 2007; Meyer *et al.*, 2012; Balsera *et al.*, 2014). Trxs *f* and *m* were proposed to play a predominant role in the redox regulation of the central biosynthetic pathways, such as the Calvin–Benson cycle, whereas Trxs *x* and *y* show a capacity to reduce peroxiredoxins (Prxs) and so were considered to have an antioxidant function (Collin *et al.*, 2003, 2004). In addition, a novel Trx, type-*z*, was identified in *Arabidopsis*, which is involved in the redox regulation of plastid transcription (Arsova *et al.*, 2010; Schröter *et al.*, 2010; Steiner *et al.*, 2011; Wimmelbacher and Börnke, 2014). Beside these canonical Trxs, several atypical Trxs have been described in the chloroplast. This is the case of HCF164, which is localized in the thylakoid membrane facing the lumen (Motahashi and Hisabori, 2006), and the small family of atypical Trxs identified in *Arabidopsis* termed AtACHTs (for atypical Cys His-rich Trxs) (Dangoor *et al.*, 2009). Finally, different Trx-like proteins were identified in chloroplasts, among which the so-called CDSP32 is the best characterized (Broin *et al.*, 2002).

In addition, chloroplasts harbour an NADPH-dependent redox system based on the activity of a bimodular enzyme consisting of an NTR with a joint Trx domain at the C-terminus, termed NTRC (Serrato *et al.*, 2004;

Kirchsteiger *et al.*, 2012). NTRC is able to conjugate both NTR and Trx activities for the efficient reduction of 2-Cys Prxs (Pérez-Ruiz *et al.*, 2006; Moon *et al.*, 2006; Alkhalifioui *et al.*, 2007), thus suggesting an antioxidant function for this enzyme (Puerto-Galán *et al.*, 2013). Additional reports indicate a function of NTRC in the redox regulation of starch synthesis (Michalska *et al.*, 2009; Lepistö *et al.*, 2013) and in different reactions of the biosynthesis of tetrapyrroles (Richter *et al.*, 2013; Pérez-Ruiz *et al.*, 2014). The high affinity of NTRC for NADPH introduces the notion that redox regulation in chloroplasts relies not only on photosynthetically reduced Fdx but also on NADPH which can be produced during the night from sugars by the oxidative pentose phosphate pathway (Spinola *et al.*, 2008; Cejudo *et al.*, 2012).

In parallel with the knowledge of the increasing complexity of the plastidial Trxs, the advance in proteomics has allowed the identification of a large number of putative targets of Trxs (Balmer *et al.*, 2003; Buchanan and Balmer, 2005; Montrichard *et al.*, 2009), which indicates that redox regulation is important for virtually any process taking place in the chloroplast. However, the question of the level of specificity or redundancy of the different Trxs in redox regulation in this organelle is still poorly understood. An *Arabidopsis* knockout mutant deficient in Trx *z* showed a severe phenotype indicating that the function of this Trx in chloroplast transcription is not redundant with other plastidial Trxs (Arsova *et al.*, 2010). By contrast, an *Arabidopsis* knockout mutant lacking Trx *x* shows almost a wild-type phenotype, indicating that this deficiency is compensated for by other plastidial redox systems (Pulido *et al.*, 2010). More uncertain is the specificity of Trxs with several isoforms, such as those of type *m* or *f*, which are considered to play a relevant role in the redox regulation of photosynthetic metabolism. Trx *m4* is involved in alternative photosynthetic electron transport (Courteille *et al.*, 2013), and the simultaneous deficiency of Trxs *m1*, *m2*, and *m4* resulted in impaired photosystem II biogenesis (Wang *et al.*, 2013).

Proteomic and biochemical studies *in vitro* have shown the relevant function of type-*f* Trxs in the redox regulation of most of the enzymes of the Calvin–Benson cycle (Michelet *et al.*, 2013). In addition, an *Arabidopsis* mutant lacking Trx *f1* shows impaired light-dependent reductive activation of ADP-glucose pyrophosphorylase (AGPase) and starch turnover (Thormählen *et al.*, 2013). Surprisingly, despite the key role proposed for type-*f* Trxs in the redox regulation of chloroplast metabolism, the Trx *f1*-deficient mutant shows a wild-type phenotype (Thormählen *et al.*, 2013). Moreover, a double mutant devoid of both Trx *f1* and Trx *f2* showed a visible phenotype indistinguishable from wild-type plants (Yoshida *et al.*, 2015), suggesting that other plastidial redox systems are able to compensate for the deficiency of *f*-type Trxs. Therefore, with the aim of establishing the role of type *f* Trxs in chloroplast performance and plant growth, we generated a double knockout mutant of *Arabidopsis* devoid of Trx *f1* and Trx *f2*, and have performed the analysis of its phenotype under different growth conditions. The double mutant shows no visible phenotype, compared with wild-type plants,

when grown under long-day conditions, however, it shows retarded growth under short-day conditions which is not rescued by high light intensity. Analysis of photosynthetic parameters and changes in the redox status of FBPase and Rubisco activase in response to light showed that type-*f* Trxs are required for the rapid reduction of the Calvin–Benson cycle enzymes in response to light, a function not compensated for by other plastidial redox systems.

## Materials and methods

### Growth conditions and plant material

*Arabidopsis thaliana* wild-type (ecotype Columbia) and mutant plants were grown in soil in growth chambers under long-day (16/8 h light/dark) or short-day (8/16 h light/dark) conditions at 22 °C during the light and 20 °C during the dark periods and a light intensity of 125  $\mu\text{E m}^{-2} \text{s}^{-1}$ . For experiments addressing the effects of irradiance, plants were grown under short-day conditions at 125, 350, and 950  $\mu\text{E m}^{-2} \text{s}^{-1}$  light intensity. A homozygous line, GK-020E05-013161, with a T-DNA insertion in the *TRX f2* gene (see Supplementary Fig. S1 at JXB online) from *Arabidopsis*, termed the *trx f2* mutant, was selected by PCR analysis with the oligonucleotides described in Supplementary Table S1. This mutant was manually crossed with the *trx f1* mutant, which was previously reported by Pérez-Ruiz et al. (2014). Seeds resulting from this cross were tested for heterozygosity of the T-DNA insertions in the *TRX f1* and *TRX f2* genes. Plants were then self-crossed and double homozygous lines were identified in the progeny by PCR analysis of genomic DNA using the oligonucleotides described in Supplementary Table S1.

### RNA extraction and qRT-PCR analysis

Total RNA was extracted using the TRIreagent RNA extraction reagent (BIOLINE) and cDNA synthesis was performed with 1  $\mu\text{g}$  of total RNA using the Maxima first strand cDNA synthesis kit (Thermo Scientific) according to the manufacturer's instructions. The content of *Trx f1* and *Trx f2* transcripts was determined by real time quantitative PCR (qRT-PCR) with RNA samples extracted from seedlings. qRT-PCR was performed with oligonucleotides shown in Supplementary Table S2 in an IQ5 real-time PCR detection system (Bio-Rad) following a standard thermal profile (95 °C, 3 min, 40 cycles of 95 °C for 10 s, and 60 °C for 30 s). The relative level of each transcript was referred to the level of the *UBIQUITIN* transcript.

### Protein extraction, alkylation assays, and Western blot analysis

For protein extraction, leaves were ground in liquid nitrogen and 10% (v/v) trichloroacetic acid (TCA) was immediately added to quench thiol oxidation. Samples were incubated on ice for 20 min and then centrifuged at 16 200  $g$  at 4 °C for 10 min. The pellets were washed with acetone, resuspended in alkylation buffer (2% SDS, 50 mM TRIS–HCl pH 7.8, 2.5% glycerol, and 4 M urea) with 10 mM methyl-maleimide polyethylene glycol (MM-PEG<sub>24</sub>) and incubated for protein thiol alkylation for 20 min at room temperature. Samples were subjected to SDS-PAGE (9.5% polyacrylamide), transferred on to nitrocellulose membranes, and probed with an anti-FBPase antibody which was kindly provided by Dr M Sahrawy, Estación Experimental del Zaidín, Granada, Spain, or with an anti-Rubisco activase antibody which was kindly provided by Dr AR Portis, USDA, Urbana, USA. The anti-*Trx f* antibody was raised by rabbit immunization with purified recombinant *Trx f1* from *Arabidopsis* at the Servicio de Producción Animal, University of Seville, Spain. This antibody also detected *Trx f2* although with somewhat lower efficiency (see Supplementary Fig. S2).

### Measurements of chlorophyll *a* fluorescence and $P_{700}$ absorbance

Room temperature chlorophyll fluorescence was measured using a pulse-amplitude modulation fluorimeter (DUAL-PAM-100, Walz, Effeltrich, Germany). The maximum PSII quantum yield, determined as variable fluorescence ( $F_v$ ) to maximal fluorescence ( $F_m$ ),  $F_v/F_m$ , was measured after the dark adaptation of the plants for 30 min and a single saturating pulse of red (635 nm) light at 10 000  $\mu\text{E m}^{-2} \text{s}^{-1}$  was applied. Induction-recovery curves were performed using red (635 nm) actinic light at 75  $\mu\text{E m}^{-2} \text{s}^{-1}$  for 8 min. Saturating pulses of red light at 10 000  $\mu\text{E m}^{-2} \text{s}^{-1}$  intensity and 0.6 s duration were applied every 60 s and recovery in darkness was recorded for up to 10 min. The parameters  $Y(\text{II})$  and  $Y(\text{NPQ})$  corresponding to the respective quantum yields of PSII photochemistry and non-photochemical quenching (NPQ) were calculated by the DUAL-PAM-100 software according to the equations in Kramer et al. (2004). Relative linear electron transport rates were measured in leaves of pre-illuminated plants by applying stepwise increasing actinic light intensities up to 2 000  $\mu\text{E m}^{-2} \text{s}^{-1}$ . The redox state of photosystem I  $P_{700}$  was monitored by following the changes in absorbance at 830 nm versus 875 nm using the DUAL-PAM-100. Plants were kept in the dark for 30 min and then, to probe the maximum extent of  $P_{700}$  oxidation, leaves were illuminated with far red (730 nm) light superimposed on the actinic light. Thereafter, absorbance traces were recorded during a 5 min illumination with 126  $\mu\text{E m}^{-2} \text{s}^{-1}$  red (635 nm) actinic light followed by 5 min darkness. Saturating pulses of red light at 10 000  $\mu\text{E m}^{-2} \text{s}^{-1}$  were applied every 20 s. The quantum yields of PSI photochemistry  $Y(\text{I})$ , donor side limitations  $Y(\text{ND})$ , and acceptor side limitations  $Y(\text{NA})$  were based on saturating pulse analysis and calculated by the DUAL-PAM-100 software.

### Determination of the rate of carbon assimilation $A_N$

Net  $\text{CO}_2$  assimilation rate ( $A_N$ ) was measured using an open gas exchange system Li-6400 equipped with the chamber head (Li-6400–40). All measurements were conducted in dark-adapted leaves of short-day grown plants (50 d-old) at 500  $\mu\text{mol mol}^{-1}$  of  $\text{CO}_2$ , a constant leaf temperature of 20 °C, and a vapour pressure deficit between leaf and air of below 1 kPa. Before the light, at an intensity of 70  $\mu\text{E m}^{-2} \text{s}^{-1}$ , was turned on in the leaf chamber,  $A_N$  was recorded for 30 min every 5 s, then recording continued until equilibrium was reached. Six leaves were measured per line.

### Determination of chlorophylls

Leaf discs were weighed and incubated in 1 ml methanol overnight at 4 °C. After extraction, chlorophyll levels were measured spectrophotometrically, as described in Porra et al. (1989), and normalized to fresh weight or leaf area. The values were compared with a Tukey Test (Anova) using a confidence interval of 99%.

### Determination of starch content

Starch content was determined in leaves of wild-type and the *Trx f*-deficient mutant grown under long-day conditions harvested before flowering (22–26-d-old), essentially as described in Lin et al. (1988). For starch extraction, leaves (100–200 mg fresh weight) harvested at the end of the day were ground in liquid nitrogen and washed with 80% (v/v) ethanol in 10 mM HEPES pH 7.6, for 2 h at 80 °C before being washed with the same solution at room temperature until the tissue was free of pigments. Dry pellets, after centrifugation, were resuspended in 1 ml of 0.2 N KOH and heated at 100 °C for 30 min. After cooling, samples were centrifuged at 17 000  $g$  for 10 min and the supernatant was adjusted to pH 5.0 with 1 N acetic acid. An aliquot of 200  $\mu\text{l}$  of this solution was used to determine the amount of starch using the enzymatic method described by Lin et al. (1988). The values were compared with a Tukey Test (Anova) using a confidence interval of 99%.

## Results

### *Type-f Trxs are dispensable for plant growth*

The *Arabidopsis* genome encodes two isoforms of *f*-type Trxs, *f1* and *f2*. It was recently reported that *Arabidopsis* knockout mutants lacking either *Trx f1* (Thormählen *et al.*, 2013) or both *Trx f1* and *Trx f2* (Yoshida *et al.*, 2015) show a wild-type phenotype with respect to growth and pigmentation. These results suggest that the loss of *f*-type Trxs might be compensated for by other plastidial redox systems. To address this issue in more detail, we have generated a double knockout mutant of *Arabidopsis* devoid of both *Trx f1* and *Trx f2* and have analysed its growth under different conditions. To that end, the *Arabidopsis* line (GK-020E05-013161) with a T-DNA insertion at the AT5G16400.1 locus encoding *Trx f2* was isolated (Supplementary Fig. S1). This line was manually crossed with the *Trx f1* knockout mutant (SALK\_128365.45.75.x) previously reported by our group (Pérez-Ruiz *et al.*, 2014), which was also characterized by Thormählen *et al.* (2013). Plants homozygous for both T-DNAs were selected by PCR analysis of genomic DNA (Supplementary Fig. S1). The double mutant, here termed *trx1f2*, was effectively devoid of both *Trx f1* and *Trx f2* as shown by the lack of transcripts of the two genes, based on qRT-PCR (Fig. 1A), and the corresponding polypeptides, as shown by Western blots probed with an antibody raised against *Trx f1* (Fig. 1B), which also cross-reacted with *Trx f2* (Supplementary Fig. S2). These results confirmed that *Trx f1* is much more abundant than *Trx f2* in wild-type plants. In addition, we tested whether the absence of type-*f* Trxs had any effect on the expression of other plastidial redox systems, but only minor differences in the levels of the transcripts of genes encoding NTRC, type-*m* and *x* Trxs were detected (see Supplementary Fig. S3).

The *trx1f2* double mutant, like the single mutants *trx1f1* and *trx1f2*, showed the wild-type phenotype when grown under the long-day photoperiod (Fig. 2A), as confirmed by the weight of the rosette leaves (Fig. 2B) and leaf chlorophyll content (Fig. 2C) of mature plants immediately before bolting. To analyse in more detail the effect of *Trx f* deficiency on plant growth, the different lines were grown under short-day conditions. Wild-type and *Trx f*-deficient mutants showed an indistinguishable growth rate up to the stage of young rosette leaves (34 d of growth), as determined by fresh weight (Fig. 3A, B). However, after 53 d of growth, the double mutant displayed a significant growth inhibition, as shown by the lower weight of rosette leaves (Fig. 3B), although the chlorophyll content was unaffected (Fig. 3C). Data of the long growth period, 53 d, are only shown for short-day (Fig. 3) and not for long-day conditions (Fig. 2), because the plant developmental stages, adult plants before bolting and advanced leaf senescence, respectively, are not comparable. We then analysed the effect of different light intensities on these mutants grown under short-day conditions. While at 125 and 350  $\mu\text{E m}^{-2} \text{s}^{-1}$  light intensity no difference was observed between the wild type and the mutant lines after 34 d of growth, *Trx f*-deficient mutants grown at 950  $\mu\text{E m}^{-2} \text{s}^{-1}$  light intensity displayed lower rosette weights than the wild-type plants (Fig. 4A, B). At high light intensity the leaf chlorophyll content was decreased, but no

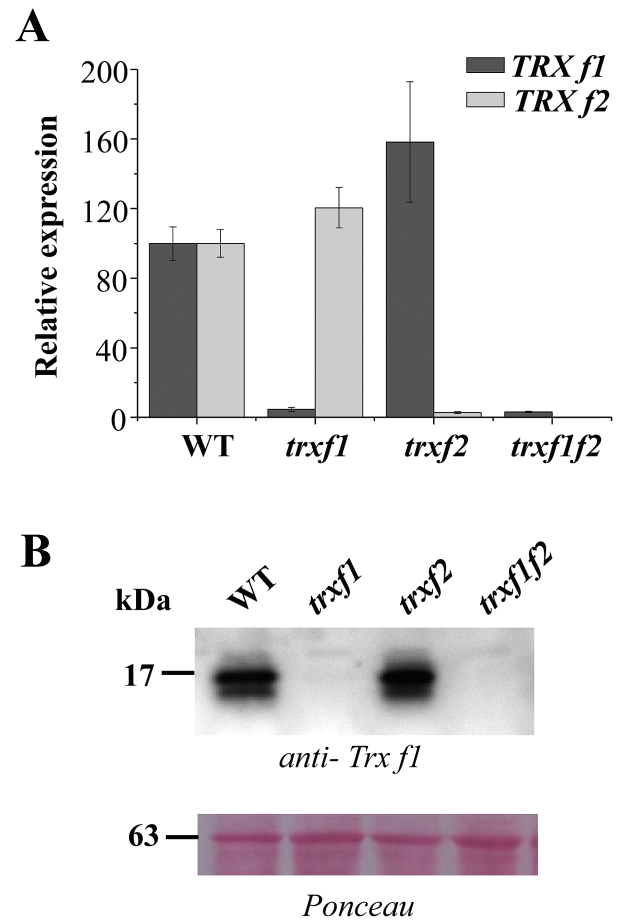


**Fig. 1.** The level of *Trx f1* and *Trx f2* transcripts and proteins in wild-type and mutant plants. (A) The content of *Trx f1* and *f2* transcripts was determined by qRT-PCR from total RNA, which was extracted from wild-type, *trx1f1*, *trx1f2*, and *trx1f2* seedlings. The pairs of oligonucleotides used for cDNA amplification are indicated in Supplementary Table S2. Transcript levels were normalized to *UBIQUITIN* amplification and referred to the level of *TRX f1* and *TRX f2* in wild-type plants. Determinations were performed three times and mean values  $\pm$ SD are represented. (B) Western blot analysis of the content of type-*f* Trxs in wild-type and mutant plants. Proteins were extracted from leaves (100 mg fresh weight) of wild-type, *trx1f1*, *trx1f2*, and *trx1f2* plants grown under short-day conditions and subjected to SDS-PAGE (13% polyacrylamide) under reducing conditions, transferred to a nitrocellulose membrane, and probed with an anti-*Trx f1* antibody. Ponceau staining was used as a loading control. Molecular weight markers in kDa are indicated on the left.

significant differences were observed between wild-type and mutant plants (Fig. 4C). Therefore, despite the central function previously attributed to type *f* Trxs in the redox regulation of chloroplast metabolism, these Trxs are dispensable for plant growth under the long-day photoperiod. Nevertheless, the retarded growth of the *trx1f2* double mutant under the short-day photoperiod at adult plant stages, even under high light conditions, confirms the light-dependent participation of *f*-type Trxs in chloroplast photosynthetic metabolism.

### *Activation of photosynthesis upon a dark–light transition is retarded in plants lacking type f Trxs*

To explore the function of *f*-type Trxs in chloroplast metabolism, different photosynthetic parameters of plants lacking either or both of the *Trx f* enzymes were first examined

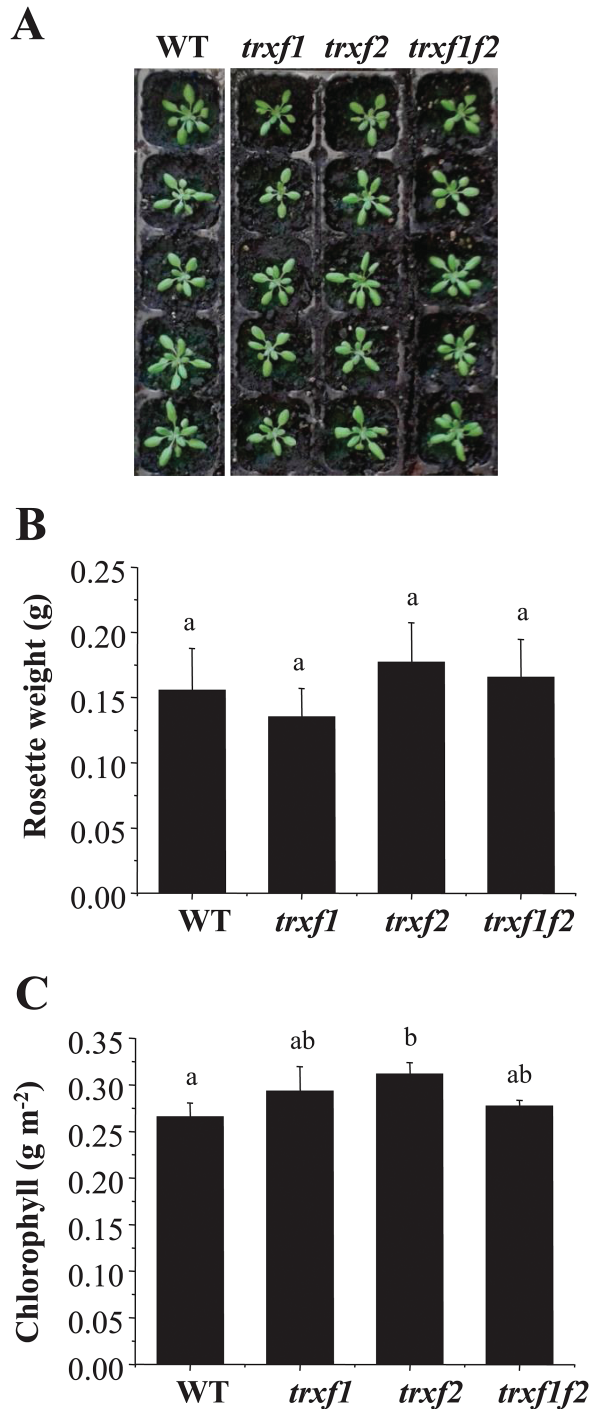


**Fig. 2.** Growth of *Arabidopsis* lines lacking type-*f* Trxs under a long-day photoperiod. (A) Plants of the wild type and mutant lines grown under long-day conditions (16/8 h light/dark, light intensity  $125 \mu\text{E m}^{-2} \text{s}^{-1}$ ) for 22 d. (B) The weight of the rosette leaves was determined from nine plants, except for the *trx1f2* double mutant which was determined from 14 plants. (C) Chlorophyll content was determined from leaf discs ( $n=6$ ) and average values  $\pm$ SD are represented. Letters indicate significant differences with the Tukey Test and a confidence interval of 99%.

using chlorophyll fluorescence. The integrity of PSII, determined as the ratio of variable to maximal fluorescence in dark-adapted leaves, was not affected in the single or double *trx1f2* mutants (Table 1). Non-photochemical quenching (NPQ) is a loss of chlorophyll fluorescence in the light

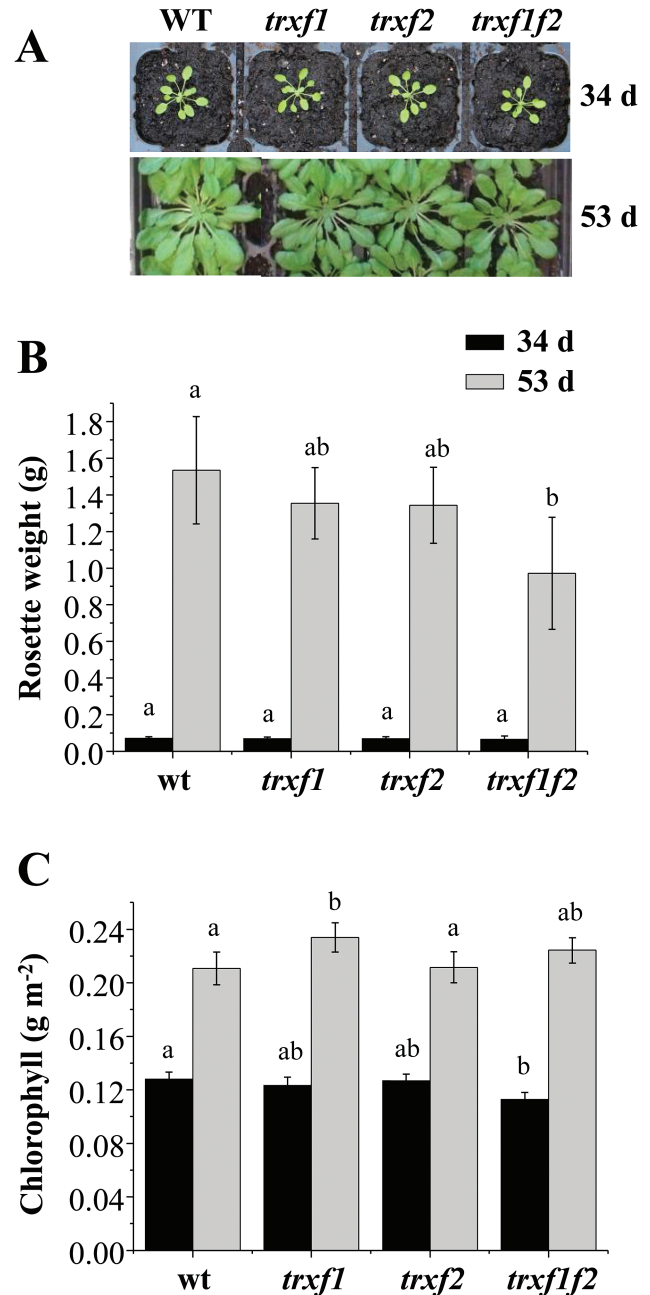


**Fig. 3.** Growth of *Arabidopsis* lines lacking type-*f* Trxs under a short-day photoperiod. (A) Representative plants of the wild type and mutant lines grown under short-day conditions (8/16 h light/dark, light intensity  $125 \mu\text{E m}^{-2} \text{s}^{-1}$ ) for 34 d and 53 d. (B) The weight of the rosette leaves was determined from 12 plants (34 d of growth) or seven plants (53 d of growth), except for the *trx1f2* double mutant which was determined from 14 plants in both cases. (C) Chlorophyll content was determined from leaf discs ( $n=6$ ). Average values  $\pm$ SD are represented. Letters indicate significant differences with the Tukey Test and a confidence interval of 99%.

which is not due to photochemistry and reflects adaptation mechanisms regulating the fraction of absorbed light that reaches the PSII reaction centre (Szabó *et al.*, 2005; Baker, 2008). The energy-dependent quenching,  $qE$ , which involves thermal dissipation of the absorbed light energy, is the main component of NPQ in plants under moderate light intensities and depends on the proton gradient across the thylakoid membrane (Szabó *et al.*, 2005; Baker, 2008; Ruban *et al.*,

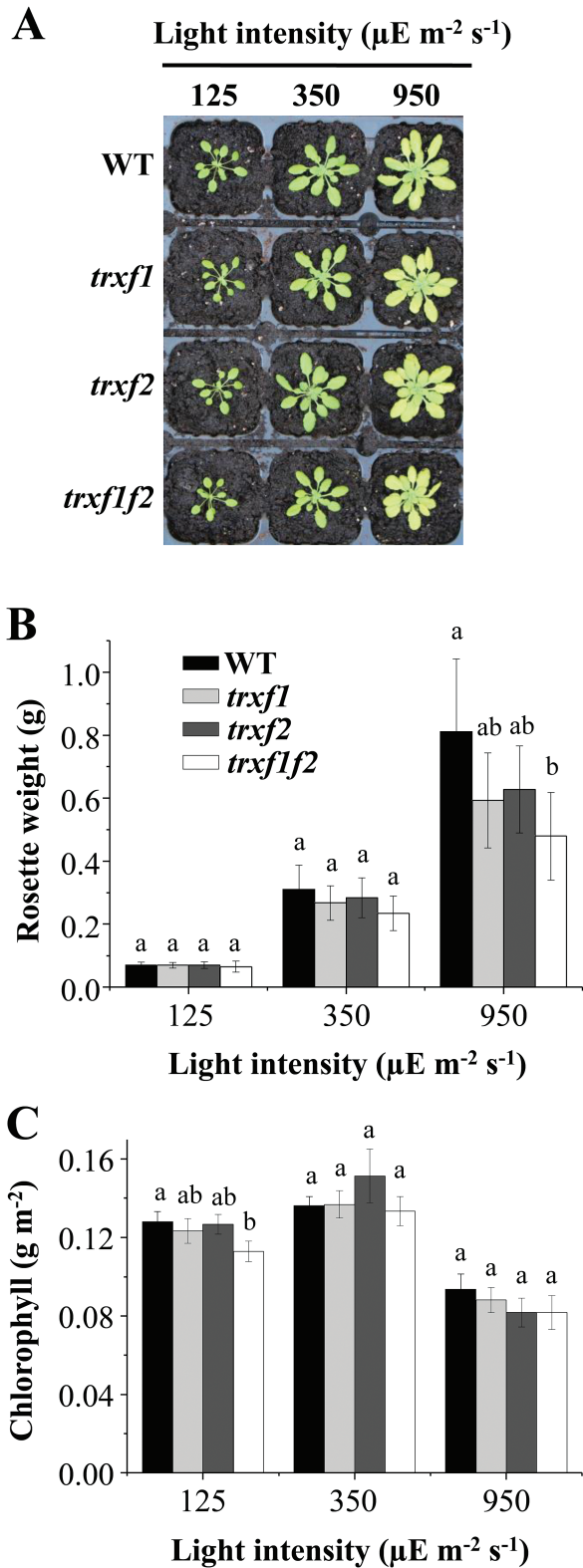


**Fig. 4.** Effect of light intensity on growth of *Arabidopsis* lines lacking type-*f* Trxs under a short-day photoperiod. (A) Representative plants of the wild type and mutant lines grown under short-day conditions (8/16h light/dark) for 34 d at increased light intensities, as indicated. (B) The weight of the rosette leaves from all lines was determined from 12 plants. (C) Chlorophyll content was determined from leaf discs ( $n=6$ ). Average values  $\pm$ SD are represented. Letters indicate significant differences with the Tukey Test and a confidence interval of 99%.

**Table 1.**  $F_v/F_m$  and kinetics of response of net  $\text{CO}_2$  assimilation rate to light

Genotype	WT	<i>trxf1</i>	<i>trxf2</i>	<i>trxf1f2</i>
$F_v/F_m$	$0.81 \pm 0.01$	$0.82 \pm 0.01$	$0.81 \pm 0.01$	$0.82 \pm 0.01$
$t_{1/2}$ (s)	$106.0 \pm 2.3$ a	$187.9 \pm 7.5$ b	$134.3 \pm 9.5$ a	$237.2 \pm 10.1$ c

The maximum PSII quantum yield was determined as variable fluorescence ( $F_v$ ) to maximal fluorescence ( $F_m$ ),  $F_v/F_m$ , in dark-adapted leaves of plants grown under short-day conditions. The  $F_v/F_m$  values ( $\pm$ SD) are the average of 12 measurements.  $t_{1/2}$  represents the time to achieve 50% of the final rate of  $\text{CO}_2$  assimilation, as shown in the data of Supplementary Fig. S5. Data presented are the means ( $\pm$ SE;  $n=6$ ). The differences between mutants and the wild type, when significant, are indicated by different letters ( $P < 0.01$ ; Anova, Tukey test).

2012). Following the onset of actinic light at low or moderate intensity, a brief peak of NPQ is normally observed in wild-type plants due to transient acidification of the thylakoid lumen before activation of photosynthesis (Kalituhno *et al.*, 2007). Such an initial peak of NPQ was also found in the *trxf2* mutant and a somewhat broader peak in the *trxf1* mutant (Fig. 5A; see Supplementary Fig. S4). By contrast, the double mutant displayed an extensive NPQ which did not relax completely even after 8 min of illumination at  $75 \mu\text{E m}^{-2} \text{s}^{-1}$  (Fig. 5A). As a result, the PSII effective quantum yield,  $Y(II)$ , increased more slowly in the light and remained lower in the *trxf1f2* double mutant (Fig. 5B). In agreement with these results, the relative linear photosynthetic electron transport rates were considerably lower in the double mutant at all light intensities examined (Fig. 6A). By contrast, only a small but significant reduction in photosynthetic electron transport rates was observed in the *trxf1* mutant, whereas the *trxf2* mutant displayed wild-type rates (Fig. 6A). Notably, the yields of NPQ were higher in *trxf1f2* plants, particularly at low light intensities (Fig. 6B). These measurements were performed using plants grown under short-day conditions and very similar results were obtained when these photosynthetic parameters were analysed in plants grown under the long-day photoperiod (see Supplementary Figs S5 and S6).

The effect of the type *f* Trxs on the control of energy quenching and photosynthetic yield might be through direct interaction with the photosynthetic apparatus or an indirect consequence of limited biosynthesis and demand for ATP, leading to lower luminal pH. The latter case should be revealed by a lower rate of consumption of electrons from photosynthetic electron transport. Therefore, we measured the PSI quantum yield,  $Y(I)$ , based on  $P_{700}$  absorbance changes, in mutant and wild-type plants (Fig. 7; see Supplementary Fig. S7). Indeed, the double mutant had a lower PSI activity due to prolonged limitations on the acceptor side,  $Y(NA)$ , after turning on the light (Fig. 7D). This indicates retardation of the activation of the biosynthetic processes which consume reducing equivalents derived from photosynthetic electron transport.

The response of the rate of  $\text{CO}_2$  fixation ( $A_N$ ) to illumination was more retarded in the *trxf1* than in the *trxf2* single mutant while the *trxf1f2* double mutant displayed even slower

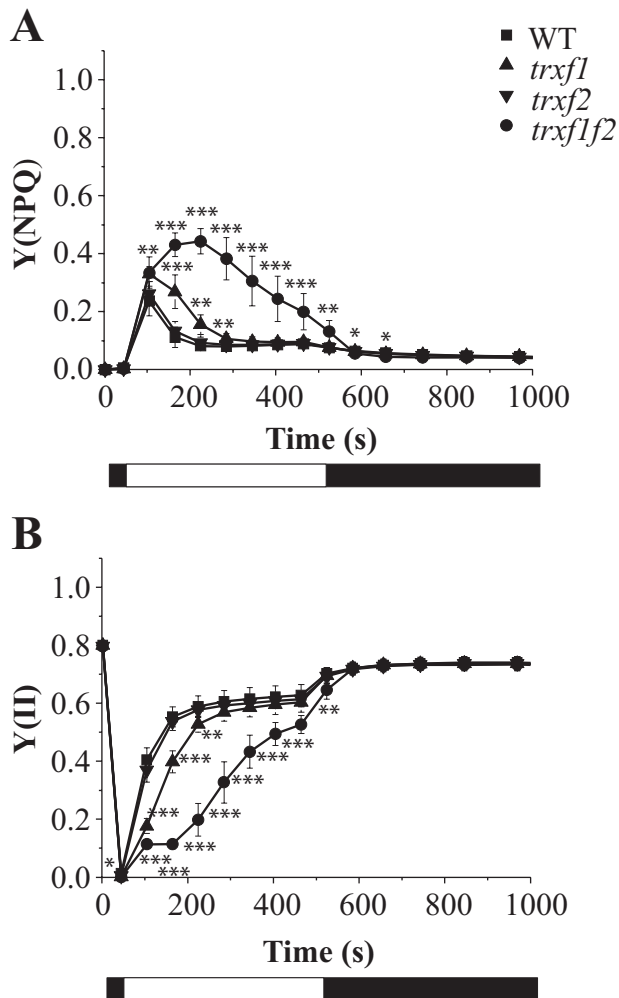


**Fig. 5.** Photosystem II activity in wild type and Trx *f*-deficient mutants. Chlorophyll fluorescence of photosystem II ( $P_{680}$ ) was measured using a pulse-amplitude modulation fluorimeter. After incubation of the plants for 30 min in darkness, an induction–recovery curve was performed to determine the quantum yields of non-photochemical quenching,  $Y(NPQ)$  (A) and photosystem II,  $Y(II)$  (B). During the 8 min induction period, a red (653 nm) actinic light at  $75 \mu\text{E m}^{-2} \text{s}^{-1}$  intensity was applied. Thereafter, the actinic light was switched off and measurements were continued for another 10 min in the dark. Saturation pulses ( $10\,000 \mu\text{E m}^{-2} \text{s}^{-1}$ , 0.6 s) every 60 s were applied. Values are the mean  $\pm$ SD of 6 plants grown for 53 d under short-day conditions. Light and dark periods are indicated by the white and black bars. Statistical significance ( $*P < 0.05$ ;  $**P < 0.01$ ;  $***P < 0.001$ ) was determined with Student's *t* test comparing values for each of the mutant lines with the wild type.

kinetics (Table 1; see Supplementary Fig. S8). The half-time for reaching the maximal  $\text{CO}_2$  fixation rate after turning on the light was more than twice as long in the double mutant compared with wild-type plants (Table 1). These results demonstrate the function of *f*-type Trxs in the rapid response of the chloroplast assimilatory metabolism to light.

#### Light-dependent reduction of FBPase and Rubisco activase is impaired in the *trxflf2* double mutant

There is extensive evidence *in vitro* supporting the relevant function of *f*-type Trxs in light-dependent reductive activation of different chloroplast enzymes including those of the

Calvin–Benson cycle (recently reviewed by Michelet *et al.*, 2013). To analyse further the function of *f*-type Trxs *in vivo*, we examined the change of the redox status of two well-known *in vitro* targets of type *f* Trxs, FBPase and Rubisco activase, in response to light in the mutant lines. To this end, samples were taken at the end of the night period from plants that had been grown at a light intensity of  $125 \mu\text{E m}^{-2} \text{s}^{-1}$  and then subjected to illumination with the same or higher ( $500 \mu\text{E m}^{-2} \text{s}^{-1}$ ) light intensity. Short-term changes of the redox status of these enzymes were analysed with the aid of the thiol-alkylating agent methyl maleimide-polyethylene glycol<sub>24</sub> (MM-PEG<sub>24</sub>), which adds 1.24 kDa per thiol group, thus producing a shift in the electrophoretic mobility of the labelled proteins that reflects their redox status. In dark-adapted plants FBPase was detected as a single band indicating that, as expected, the enzyme was fully oxidized under these conditions (Fig. 8). In wild-type plants, FBPase becomes rapidly reduced in response to light within seconds after illumination (Fig. 8). The level of reduction of FBPase proved to be dependent on light intensity since the enzyme became fully reduced after 10 min at  $500 \mu\text{E m}^{-2} \text{s}^{-1}$ , whereas the growth light intensity of  $125 \mu\text{E m}^{-2} \text{s}^{-1}$  only promoted a partial reduction, approximately 50%, of the enzyme (Fig. 8). While the deficiency of Trx *f2* exerted almost no effect on FBPase reduction in response to light, the deficiency of Trx *f1* significantly impaired the level of reduction of the enzyme at both light intensities (Fig. 8). The *trxflf2* double mutant showed not only a pronounced delay of FBPase reduction in response to light but also a lower level of reduction of the enzyme after 10 min of illumination, even at the higher light intensity tested here (Fig. 8). A similar pattern of reduction in response to light was observed for another prominent redox-regulated enzyme of the Calvin–Benson cycle, Rubisco activase (Fig. 9). In dark-adapted samples Rubisco activase was detected as a double band corresponding to isoforms of 46 and 43 kDa, respectively, due to alternative splicing. The long isoform has a C-terminal extension that includes two cysteines which may form an intramolecular disulphide that renders the enzyme inactive (Zhang and Portis, 1999).

Quantification of the reduction of FBPase and Rubisco activase from a series of experiments (such as those presented in Figs 8 and 9), revealed that the levels of reduction of both enzymes remained at 50% of the wild-type level in the *trxflf2* double mutant after 10 min illumination at the growth light intensity (see Supplementary Fig. S9A, B). Furthermore, we analysed the change of the redox status of FBPase following a light–dark transition. Re-oxidation of FBPase in the dark was faster in all three Trx *f* deficient mutants than in wild-type plants (Fig. 10). However, after 5 min darkness, FBPase was also nearly completely oxidized in the wild type (Fig. 10). Finally, we compared the starch content in leaves which was significantly lower in the *trxflf2* double mutant than in the wild type and the single mutants (Fig. 11).

## Discussion

Following the demonstration of the function of Trxs in the light-dependent regulation of chloroplast photosynthetic

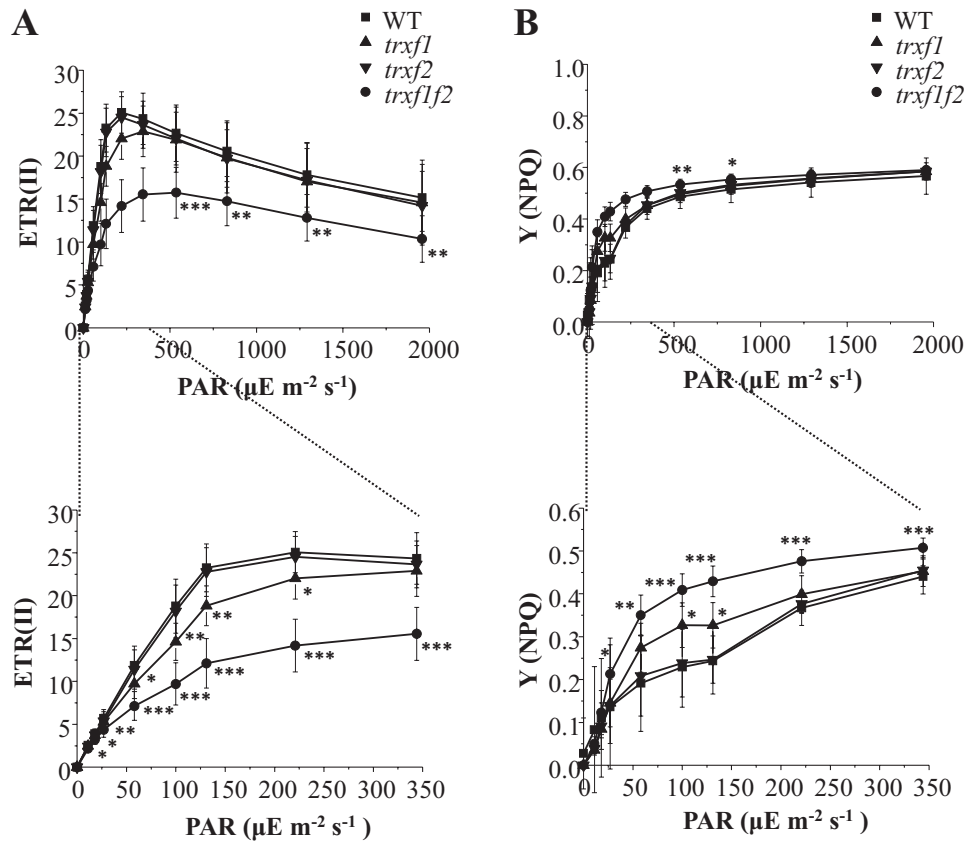


**Fig. 6.** Light-dependent linear photosynthetic electron transport and NPQ in the wild type and Trx *f*-deficient mutants. (A) Relative linear electron transport rates of photosystem II, ETR (II) was measured in pre-illuminated attached leaves of plants grown at  $125 \mu\text{E m}^{-2} \text{s}^{-1}$  under short-day conditions. Chlorophyll fluorescence of photosystem II was determined using a pulse-amplitude modulation fluorimeter. Each data point is the mean  $\pm$ SD of the ETR (II) from eight plants under short-day conditions. PAR (photosynthetically active radiation). (B) Quantum yields of NPQ from the corresponding light-titration curves in (A). Statistical significance ( $*P < 0.05$ ;  $**P < 0.01$ ;  $***P < 0.001$ ) was determined with Student's *t* test comparing values for each of the mutant lines with the wild type.

metabolism (Wolosiuk and Buchanan, 1976), extensive biochemical and proteomic work has shown the central role of *f*-type Trxs in the reductive activation of most of the Calvin–Benson cycle enzymes. In this regard, the findings that overexpression of Trx *f*, but not Trx *m*, enhanced starch accumulation and increased the content of sugars in tobacco leaves (Sanz-Barrio *et al.*, 2013) lend further support to the idea that, among the complex set of plastidial Trxs, those of type *f* play a key role in the redox regulation of carbon metabolism. However, *Arabidopsis* knockout mutants for Trx *f1*, which accounts for up to 95% of the total *f*-type Trxs in this plant, showed impairment of AGPase redox regulation and leaf diurnal starch turnover alterations, yet the visible phenotype of these mutants was indistinguishable from the wild type (Thormählen *et al.*, 2013). Moreover, double mutants lacking both Trx *f1* and *f2* were also indistinguishable from wild type plants (Yoshida *et al.*, 2015). Thus, the lack of *f*-type Trxs seems not to affect plant growth despite the relevant function proposed for these Trxs in the redox regulation of chloroplast metabolism based on biochemical analyses. These results suggest that additional redox systems may compensate for the function of *f*-type Trxs being sufficient to support the redox regulation that allows plant growth.

To address this issue, in the present work we have generated a double mutant of *Arabidopsis*, here termed *trxf1f2*, lacking both Trx *f1* and Trx *f2*. Both qRT-PCR and Western blot analyses (Fig. 1A, B) confirmed that the *trxf1f2* double mutant is a null mutant devoid of *f*-type Trxs. Western blot analysis of leaf extracts from wild-type plants detected a double band, which might correspond to *f1* and *f2* Trxs. However, this possibility was ruled out because the double band was detected in the *trxf2* mutant but not in the *trxf1* mutant. Thus, the double band is most probably indicative of a post-translational modification, the nature of which is still unknown. Under long-day conditions the growth of the single mutants, *trxf1* and *trxf2*, was indistinguishable from that of wild-type plants, consistent with previous studies on Trx *f1*-deficient mutants (Thormählen *et al.*, 2013). Similarly, the double mutant displayed the wild-type phenotype when grown under long-day conditions, as shown for type-*f* null mutants recently reported (Yoshida *et al.*, 2015). However, under short-day conditions, single mutants *trxf1* and *trxf2* showed slightly retarded growth (Fig. 3B), in agreement with the behaviour of the Trx *f1*-deficient mutant, which shows retarded growth under short-days, but not under the long-day photoperiod (Thormählen *et al.*, 2015). Adult plants of the *trxf1f2* double mutant showed retarded growth (Fig. 3)



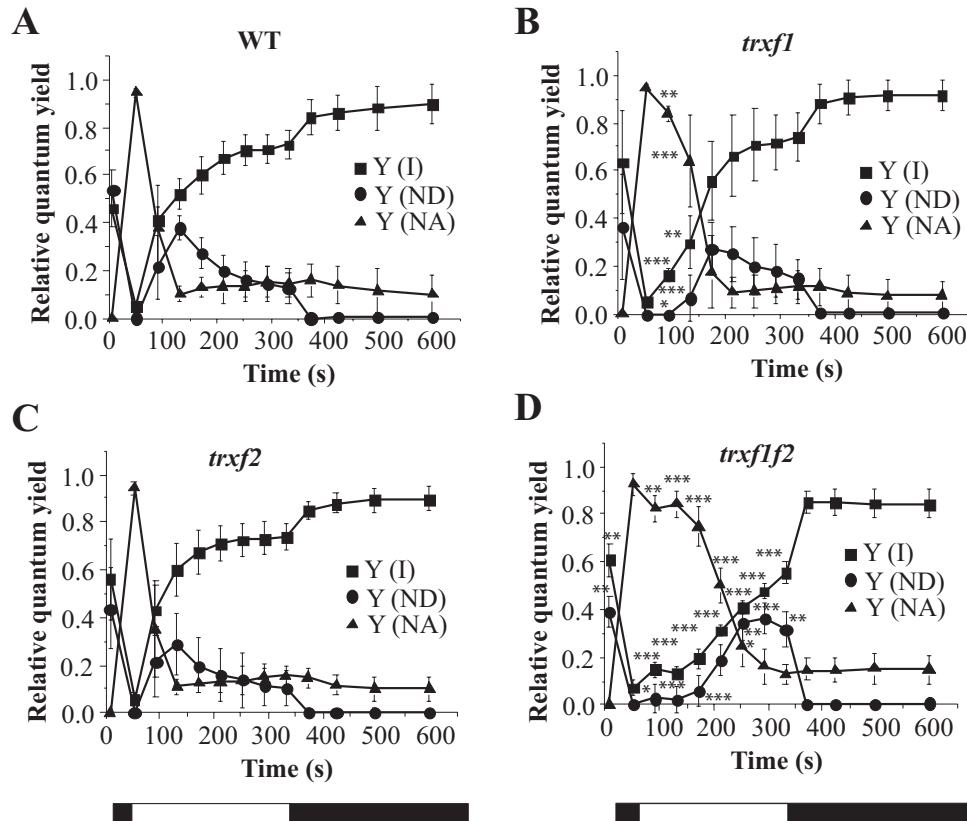


**Fig. 7.** Comparative analysis of photosystem I activity in the wild type and Trx *f*-deficient mutants. The absorbance of oxidized photosystem I ( $P_{700}$ ) at 830nm was measured using a pulse-amplitude modulation fluorimeter. The redox state of photosystem I ( $P_{700}$ ) was inferred from changes in this absorbance and monitored for 10 min. After 30 min dark adaptation (maximum  $P_{700}$  reduced), leaves were illuminated with far-red light superimposed on actinic red light ( $126 \mu\text{E m}^{-2} \text{s}^{-1}$ , 635 nm) to achieve the maximum oxidation of  $P_{700}$  and, subsequently, the actinic light was kept on for 5 min followed by another 5 min of darkness. White light saturation pulses ( $10\,000 \mu\text{E m}^{-2} \text{s}^{-1}$ , 0.6 s) were applied every 20 s. The quantum yields of PSI Y(I), donor side limitations Y(ND), and acceptor side limitations Y(NA) are based on saturating pulse analysis. Data were collected from six plants grown under short-day conditions and mean  $\pm$ SD are represented. Statistical significance (\* $P < 0.05$ ; \*\* $P < 0.01$ ; \*\*\* $P < 0.001$ ) was determined with Student's *t* test comparing values for each of the mutant lines (B, C, D) with the wild type (A).

which was observed only at later stages of development, indicating that the effect of the deficiency of *f*-type Trxs reported here (lower efficiency of photosynthetic parameters, impaired reduction of Calvin–Benson enzymes, lower starch content) requires time to affect plant growth. Most likely, the delayed growth of the *trx f*-deficient mutant under short-day conditions is not attributable to short-term kinetics of activation, but rather to the lower final level of reduction of enzymes, such as FBPase and Rubisco activase, which can be seen after 10 min of illumination (Figs 8, 9) and also at the end of the day (Fig. 10). Moreover, high light intensity ( $950 \mu\text{E m}^{-2} \text{s}^{-1}$ ), which caused the decrease in chlorophyll content of both the wild type and mutant lines (Fig. 4C), resulted in retarded growth not only of the double *trx1f2* mutant but also of the single mutants after 34 d of growth (Fig. 4B). Therefore, deficiency of *f*-type Trxs affects the plant's response to high light suggesting the participation of these Trxs in plant adaptation to light intensities that might produce oxidative stress. Therefore, despite the central function attributed to type *f* Trxs in chloroplast redox regulation based on biochemical *in vitro* analyses, the *in vivo* approach reported here shows that these Trxs are dispensable for plant growth at least under the standard long-day conditions performed in this study. It should be

noted, however, that conditions that may cause light limitation, such as growth under a short-day photoperiod, have a negative effect on the growth rate of Trx *f*-deficient mutants. Moreover, higher light intensity failed to stimulate the growth of mutant plants to the extent that it was stimulated in wild-type plants (Fig. 4), indicating the relevant function of type-*f* Trxs is for plant adaptation to varying light conditions.

The genes encoding Trx *f1* and Trx *f2* isoforms are subject to different regulation in *Arabidopsis*. The expression of the *TRX f1* gene responds to light, whereas the *TRX f2* gene is under circadian control (Barajas-López *et al.*, 2011). The differential pattern of expression of these genes might indicate different functions for the respective Trx *f* isoforms. However, all the photosynthetic parameters analysed in this study, such as photosynthetic electron transport and response to illumination of the rate of  $\text{CO}_2$  fixation ( $A_N$ ), were more affected in the *trx1f1* than in the *trx2f2* mutant, while the double mutant showed an additive effect. Most probably, these results reflect the higher content of Trx *f1* in wild-type plants (Fig. 1B) and support a redundant function for both *f*-type Trxs in *Arabidopsis*.

A relevant question concerning chloroplast redox regulation is the level of redundancy or specificity among the

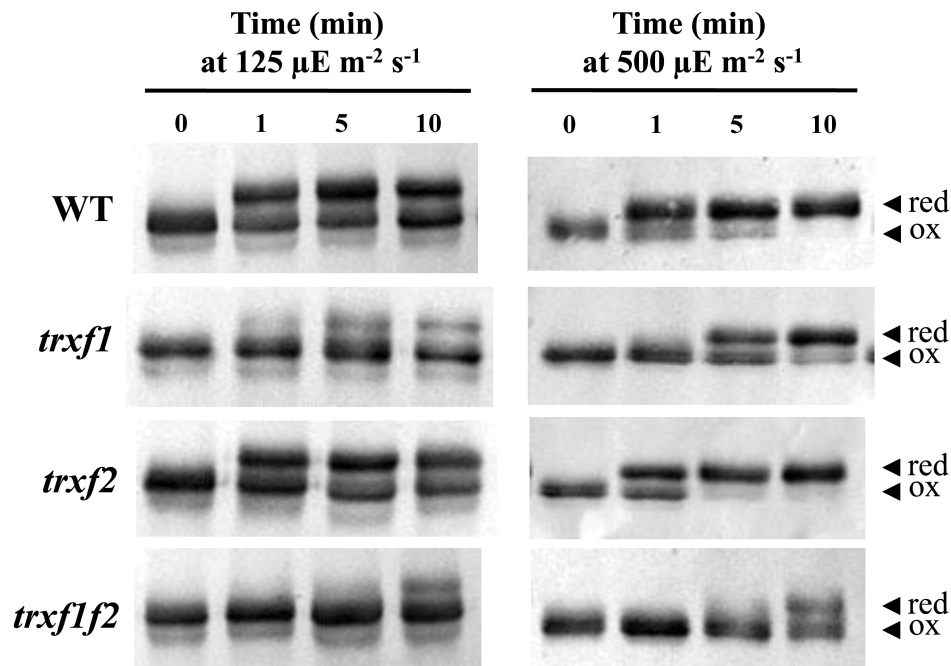


**Fig. 8.** *In vivo* redox status of FBPase in response to light in the wild type and *Trx f* mutant lines. The redox status of FBPase from the different lines under analysis, as indicated on the left, was determined in leaf extracts from plants grown under short-day conditions and harvested at the end of the dark period (time 0), and after 1, 5, and 10 min of illumination at the indicated light intensities. Total leaf proteins were extracted in the presence of 10% TCA and protein thiols were alkylated with 10 mM MM-PEG<sub>24</sub>. Proteins were resolved in SDS-PAGE (9.5% polyacrylamide) under non-reducing conditions, transferred to nitrocellulose filters, and probed with an anti-FBPase antibody; red, reduced; ox, oxidized.

many different types of Trx in this organelle. This issue is currently being addressed with the aid of mutants or transgenic plants with altered levels of the different plastidial Trxs. In this regard, the redox status *in vivo* of the Mg chelatase CHLI subunit from pea plants was affected by the simultaneous silencing of the *TRX f* and *TRX m* genes, but not by the silencing of the *TRX f* gene alone (Luo *et al.*, 2012), showing the compensatory effect of *Trx m* on the regulation of this enzyme of the chlorophyll biosynthesis pathway. Therefore, one might assume that *m*-type Trxs could substitute for *f*-type Trxs in the light-dependent redox regulation of the Calvin–Benson cycle enzymes which is in line with the relevant role proposed for *m*-type Trxs in the redox regulation of these enzymes (Okegawa and Motohashi, 2015). However, comparative analyses *in vitro* of a large number of the *Arabidopsis* plastid Trxs (*f1*, *f2*, *m1*, *m2*, *m3*, *m4*, *x*, *y1*, and *y2*) confirmed that only the *f*-type Trxs are capable of activating FBPase using recombinant enzymes (Collin *et al.*, 2003, 2004). The relevant function of *f*-type Trxs in the redox regulation of chloroplast enzymes was further confirmed by *in vivo* studies showing the incomplete reduction of FBPase in mutant plants devoid of *Trx f1* (Thormählen *et al.*, 2015) and the double mutant devoid of both *Trx f1* and *Trx f2* (Yoshida *et al.*, 2015). In addition, purified Rubisco activase has been shown to be readily reduced and activated by spinach *Trx f*, whereas spinach *Trx m* is unable to reduce this enzyme (Zhang and Portis, 1999). In line with the proposed central function of *f*-type Trxs in light-dependent redox regulation of the Calvin–Benson cycle enzymes, our studies *in vivo* show that reduction of both FBPase and Rubisco activase upon illumination is impaired in the *trxf1f2* knockout mutant

(Figs 8, 9; Supplementary Fig. S9). Nevertheless, despite the complete absence of *Trx f*, both enzymes become partially reduced during illumination. These results suggest that the *in vitro* studies showing the predominant function of *f*-type Trxs in the redox regulation of the Calvin–Benson cycle enzymes cannot be extrapolated to the physiological situation and show that the double mutant relies on alternative system(s) capable of limited reductive activation of these enzymes in response to light. In this regard, it is worth mentioning that mutant plants devoid of NTRC, an alternative chloroplast redox system, show an incomplete level of FBPase reduction, this effect being even more dramatic in the *ntrc-trxf1* double mutant (Thormählen *et al.*, 2015). Therefore, light-dependent redox regulation of Calvin–Benson cycle enzymes, such as FBPase, seems to be the result of the action of different redox systems including type-*f* Trxs (Fig. 8, this work; Thormählen *et al.*, 2015; Yoshida *et al.*, 2015), type *m* Trxs (Okegawa and Motohashi, 2015), and NTRC (Thormählen *et al.*, 2015). The finding that NTRC and *Trx f1* act in concert (Thormählen *et al.*, 2015) indicates the existence of cross-talk among these redox systems.

The light-dependent reduction of FBPase and Rubisco activase show very similar patterns in wild-type plants on the one hand and in *Trx f*-deficient plants on the other (Figs 8, 9; Supplementary Fig. S9), suggesting common regulatory mechanisms for the two enzymes. This may be significant since both enzymes are involved in the pathway of CO<sub>2</sub> fixation in the chloroplast. It should be noted that plant chloroplasts contain two types of FBPase, termed FBPase I and II, but only one of them, FBPase I, is redox-regulated (Serrato *et al.*, 2009). Our results show that, upon illumination with a

higher light intensity,  $500 \mu\text{E m}^{-2}\text{s}^{-1}$ , FBPase becomes fully reduced (Fig. 8) indicating that the redox-insensitive form, FBPase II, is present in minor amounts in chloroplasts, in agreement with previous results (Rojas-González *et al.*, 2015).

An interesting observation regarding the redox state of FBPase and Rubisco activase is that these enzymes do not become fully reduced under the growth light intensity even in wild-type plants. This is in agreement with recent reports (Yoshida *et al.* 2014, 2015) showing that *Arabidopsis* plants display only partial reduction of the FBPase when illuminated at low light intensity. However, we observed the complete reduction of FBPase in wild-type plants after 10 min illumination at  $500 \mu\text{E m}^{-2}\text{s}^{-1}$  light intensity, while the *trxf1f2* double mutant showed a partial reduction of the enzyme (Fig. 8). A remarkable implication of these results is that plants that have been adapted to low light conditions have a significant pool of inactive, not fully reduced, enzymes. A possible advantage of this seemingly wasteful synthesis of excess Calvin–Benson cycle enzymes is that, after a sudden increase in photon flux leading to higher rates of photosynthetic electron transport, the ATP and NADPH generated would immediately be utilized for carbon dioxide fixation and, thus, would not be a problem of light stress. Obviously, a prerequisite for this to occur is that there are sufficiently high amounts of *f*-type Trxs to catalyse the reductive activation of these

enzymes. In addition, we have analysed the changes of redox status of FBPase in light–dark transitions. Re-oxidation of FBPase in response to darkness is again a very rapid process which is essentially completed in 5 min in wild-type plants (Fig. 10). The fact that re-oxidation is faster in the mutants could indicate that, until exhausted, a pool of reduced *f*-type Trxs continues to catalyse reduction in the dark.

Light-harvesting efficiency and photosynthetic electron transport are highly sensitive to changes in carbon assimilation. For example, sub-atmospheric levels of  $\text{CO}_2$ , which result in limited regeneration of ADP and  $\text{NADP}^+$ , lead to elevated NPQ and decreased effective PSII quantum yield at low or moderate light intensities (Kramer *et al.*, 2004). Similarly, inhibition of the Calvin–Benson cycle enzymes *in vivo* by iodoacetamide leads to higher NPQ and slower linear photosynthetic electron transport (Joliot and Alric, 2013). Notably, the *qE* component of NPQ ensures safe dissipation of the light energy absorbed and prevents excess excitation of PSII (Szabó *et al.*, 2005; Baker, 2008; Ruban *et al.*, 2012). Such a negative feedback control that arises from hampered  $\text{CO}_2$  fixation is the most likely explanation for the results concerning the activities of PSII and PSI obtained from the *trxf1f2* mutant plants using chlorophyll fluorescence and  $\text{P}_{700}$  absorbance. Hence, despite normal maximum PSII quantum

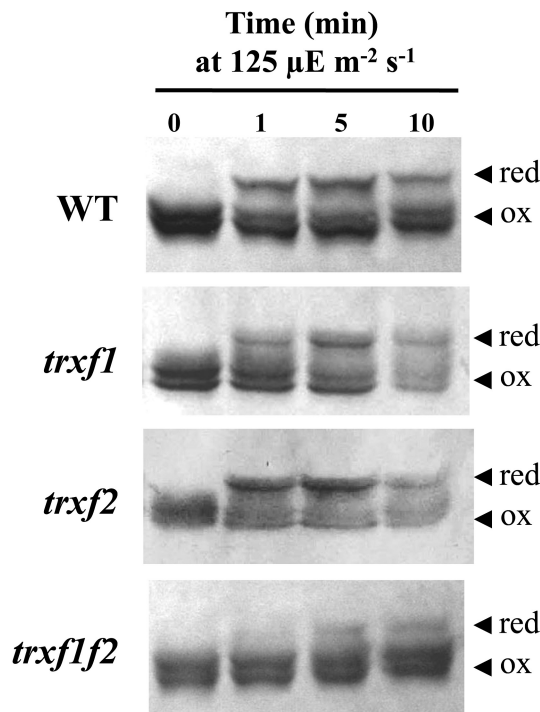


**Fig. 9.** *In vivo* redox status of Rubisco activase in response to light in the wild type and Trx *f* mutant lines. The redox status of Rubisco activase from the different lines under analysis, as indicated on the left, was determined in leaf extracts from plants grown under short-day conditions and harvested at the end of the dark period (time 0), and after 1, 5, and 10 min of illumination. Total leaf proteins were extracted in the presence of 10% TCA and protein thiols were alkylated with 10 mM MM-PEG<sub>24</sub>. Samples were fractionated in SDS-PAGE (9.5% polyacrylamide) under non-reducing conditions, transferred to nitrocellulose filters, and probed with an anti-Rubisco activase antibody; red, reduced; ox, oxidized.

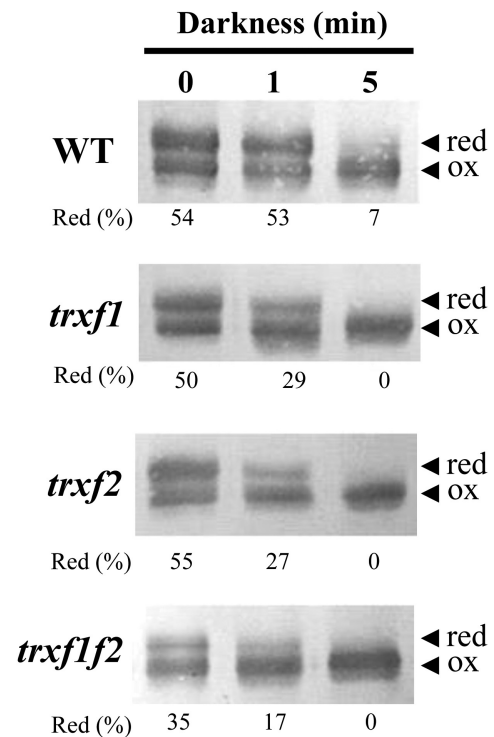


**Fig. 10.** Re-oxidation of FBPase in response to darkness. The redox status of FBPase from the different lines under analysis, as indicated on the left, was determined in leaf extracts from plants grown under short-day conditions and harvested at the end of the light period (time 0), and after 1 min and 5 min of darkness. Total leaf proteins were extracted in the presence of 10% TCA and protein thiols were alkylated with 10 mM MM(PEG)<sub>24</sub>. Proteins were resolved in SDS-PAGE (9.5% polyacrylamide) under non-reducing conditions, transferred to nitrocellulose filters, and probed with an anti-FBPase antibody; red, reduced; ox, oxidized. Band intensities were quantified and the percentage of reduced FBPase is indicated.

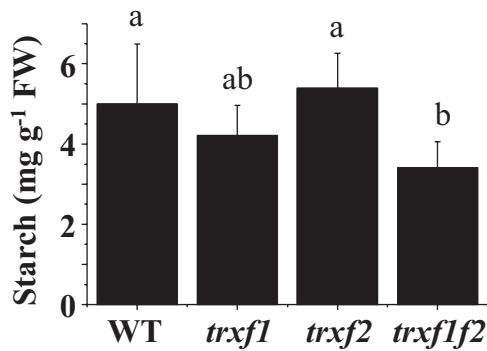


**Fig. 11.** The content of starch in leaves of the wild type and *Trx f* mutant lines. Starch content was determined at the end of the day in leaves from plants grown under long-day conditions for 22–26 d. Data are the mean  $\pm$ SD of five replicates from two different experiments (with a total of three starch extractions). Letters indicate significant differences with the Tukey Test and a confidence interval of 99%.

efficiency,  $F_v/F_m$ , the linear photosynthetic electron transport rate is significantly decreased in the double *trxfl1f2* knockout mutant compared with the wild type, particularly at lower light intensities. At 100–150  $\mu\text{E m}^{-2} \text{s}^{-1}$ , which corresponds to growth light intensity, the electron transport in the double mutant was only half that in wild-type plants (Fig. 6A) and the yield of NPQ was twice as high (Fig. 6B).

Although in plants devoid of *f*-type Trxs the response of the rate of carbon assimilation ( $A_N$ ) to light was delayed (Table 1) these plants still reached carbon assimilation rates similar to those of the wild type (Supplementary Fig. S8). However, the content of starch was diminished in the *trxfl1f2* mutant (Fig. 11) which is in line with the impaired activation of the AGPase of the *trxfl1* single mutant (Thormählen *et al.*, 2013). Nevertheless, the leaf starch accumulated during the day under a long-day light regime seems sufficient for the correspondingly short night and to support wild-type growth rates (Fig. 2).

## Conclusion

In summary, the *in vivo* approach undertaken in this work identifies the impact of type *f* Trxs on photosynthetic performance in *Arabidopsis*, such as the kinetics of activation of carbon assimilation, the redox status of Calvin–Benson cycle enzymes upon a dark–light transition, and the control of photosynthetic electron transport. The fact that these parameters were impaired in plants devoid of type *f* Trxs indicates that the functions of these Trxs are specific and are not compensated for by other Trxs or chloroplast redox systems. On the other hand, FBPase and Rubisco activase showed a significant level of reduction upon dark–light transition in the *trxfl1f2* double mutant indicating that additional chloroplast redox systems participate in light-dependent reduction of these Calvin–Benson cycle enzymes. This stands out against the well-established notion, based on biochemical *in vitro* analyses, of the almost exclusive role attributed to type *f* Trxs in the redox regulation of these enzymes. Surprisingly, the growth of plants devoid of type *f* Trxs is indistinguishable

from wild-type plants when grown under standard conditions with a long-day photoperiod, indicating that the function of type *f* Trxs are dispensable for growth.

## Supplementary data

Supplementary data can be found at *JXB* online.

**Table S1.** Sequence of oligonucleotides used for genotype analyses.

**Table S2.** Sequence of oligonucleotides used for gene expression analyses.

**Figure S1.** Genotype of *Trx f*-deficient mutants.

**Figure S2.** Cross-reaction of the anti *Trx fl* antibody with *Trx fl* and *Trx f2*.

**Figure S3.** Level of *NTRC*, *m*- and *x*-type *TRX* gene transcripts in *Trx f*-deficient mutants.

**Figure S4.** Chlorophyll *a* fluorescence of PSII.

**Figure S5.** Photosystem II activity in wild type and *Trx f* deficient mutants grown under long-day conditions.

**Figure S6.** Light-dependent linear photosynthetic electron transport and NPQ in wild type and *Trx f* deficient mutants grown under long-day conditions.

**Figure S7.** Absorbance of the oxidized form of PSI.

**Figure S8.** Net  $\text{CO}_2$  assimilation rate ( $A_N$ ) in the wild type and *Trx f* deficient mutants.

**Figure S9.** Light-dependent reduction FBPase and Rubisco activase.

## Acknowledgements

This work was supported by grant number BIO2013-43556-P from the Ministerio de Economía y Competitividad, Spain. The anti-FBPase and anti-Rubisco activase antibodies were provided by Dr Sahrawy, Estación Experimental del Zaidín, Granada, Spain and by Dr Portis, USDA, Urbana, USA, respectively. BN was the recipient of an FPI pre-doctoral fellowship from the Ministerio de Economía y Competitividad, Spain.

## References

- Alkhalifioui F, Renard M, Montrichard F. 2007. Unique properties of NADP-thioredoxin reductase C in legumes. *Journal of Experimental Botany* **58**, 969–978.
- Arsova B, Hoja U, Wimmelbacher M, Greiner E, Ustün S, Melzer M, Petersen K, Lein W, Börnke F. 2010. Plastidial thioredoxin *z* interacts with two fructokinase-like proteins in a thiol-dependent manner: evidence for an essential role in chloroplast development in *Arabidopsis* and *Nicotiana benthamiana*. *The Plant Cell* **22**, 1498–1515.
- Baker N. 2008. Chlorophyll fluorescence: a probe of photosynthesis *in vivo*. *Annual Review of Plant Biology* **59**, 89–113.
- Balmer Y, Koller A, del Val G, Manieri W, Schürmann P, Buchanan BB. 2003. Proteomics gives insight into the regulatory function of chloroplast thioredoxins. *Proceedings of the National Academy of Sciences, USA* **100**, 370–375.
- Balsera M, Uberegui E, Schürmann P, Buchanan BB. 2014. Evolutionary development of redox regulation in chloroplasts. *Antioxidants and Redox Signaling* **20**, 1327–1355.
- Barajas-López J, Serrato AJ, Cazalis R, Meyer Y, Chueca A, Reichheld JP, Sahrawy M. 2011. Circadian regulation of chloroplastic *f* and *m* thioredoxins through control of the CCA1 transcription factor. *Journal of Experimental Botany* **62**, 2039–2051.
- Broin M, Cuié S, Eymery F, Rey P. 2002. The plastidic 2-cysteine peroxidoxin is a target for a thioredoxin involved in the protection of the

- photosynthetic apparatus against oxidative damage. *The Plant Cell* **14**, 1417–1432.
- Buchanan BB, Balmer Y.** 2005. Redox regulation: a broadening horizon. *Annual Review of Plant Biology* **56**, 187–220.
- Buchanan BB, Holmgren A, Jacquot JP, Scheibe R.** 2012. Fifty years in the thioredoxin field and a bountiful harvest. *Biochimica et Biophysica Acta* **1820**, 1822–1829.
- Cejudo FJ, Ferrández J, Cano B, Puerto-Galán L, Guinea M.** 2012. The function of the NADPH thioredoxin reductase C-2-Cys peroxiredoxin system in plastid redox regulation and signalling. *FEBS Letters* **586**, 2974–2980.
- Chibani K, Wingsle G, Jacquot JP, Gelhaye E, Rouhier N.** 2009. Comparative genomic study of the thioredoxin family in photosynthetic organisms with emphasis on *Populus trichocarpa*. *Molecular Plant* **2**, 308–322.
- Collin V, Issakidis-Bourguet E, Marchand C, Hirasawa M, Lancelin J-M, Knaff DB, Miginiac-Maslow M.** 2003. The *Arabidopsis* plastidial thioredoxins. New functions and new insights into specificity. *Journal of Biological Chemistry* **278**, 23747–23752.
- Collin V, Lamkemeyer P, Miginiac-Maslow M, Hirasawa M, Knaff DB, Dietz KJ, Issakidis-Bourguet E.** 2004. Characterization of plastidial thioredoxins from *Arabidopsis* belonging to the new  $\gamma$ -type. *Plant Physiology* **136**, 4088–4095.
- Courteille A, Vesa S, Sanz-Barrio R, Cazalé AC, Becuwe-Linka N, Farran I, Havaux M, Rey P, Rumeau D.** 2013. Thioredoxin m4 controls photosynthetic alternative electron pathways in *Arabidopsis*. *Plant Physiology* **161**, 508–520.
- Dai S, Friemann R, Glauser DA, Bourquin F, Manieri W, Schürmann P, Eklund H.** 2007. Structural snapshots along the reaction pathway of ferredoxin-thioredoxin reductase. *Nature* **448**, 92–96.
- Dangoor I, Peled-Zehavi H, Levitan A, Pasand O, Danon A.** 2009. A small family of chloroplast atypical thioredoxins. *Plant Physiology* **149**, 1240–1250.
- Jacquot JP, Eklund H, Rouhier N, Schürmann P.** 2009. Structural and evolutionary aspects of thioredoxin reductases in photosynthetic organisms. *Trends in Plant Science* **14**, 336–343.
- Jarvis P, López-Juez E.** 2013. Biogenesis and homeostasis of chloroplasts and other plastids. *Nature Reviews Molecular and Cellular Biology* **14**, 787–802.
- Joliet P, Alric J.** 2013. Inhibition of CO<sub>2</sub> fixation by iodoacetamide stimulates cyclic electron flow and non-photochemical quenching upon far-red illumination. *Photosynthesis Research* **115**, 55–63.
- Kalituho L, Beran KC, Jahns P.** 2007. The transiently generated nonphotochemical quenching of excitation energy in *Arabidopsis* leaves is modulated by zeaxanthin. *Plant Physiology* **143**, 1861–1870.
- Kirchsteiger K, Ferrández J, Pascual MB, González M, Cejudo FJ.** 2012. NADPH thioredoxin reductase C is localized in plastids of photosynthetic and nonphotosynthetic tissues and is involved in lateral root formation in *Arabidopsis*. *The Plant Cell* **24**, 1534–1548.
- Kramer DM, Johnson G, Kiirats O, Edwards GE.** 2004. New fluorescence parameters for the determination of Q<sub>A</sub> redox state and excitation energy fluxes. *Photosynthesis Research* **79**, 209–218.
- Lemaire SD, Michelet L, Zaffagnini M, Massot V, Issakidis-Bourguet E.** 2007. Thioredoxins in chloroplasts. *Current Genetics* **51**, 343–365.
- Lepistö A, Pakula E, Toivola J, Krieger-Liszky A, Vignols F, Rintamäki E.** 2013. Deletion of chloroplast NADPH-dependent thioredoxin reductase results in inability to regulate starch synthesis and causes stunted growth under short-day photoperiods. *Journal of Experimental Botany* **64**, 3843–3854.
- Lin TP, Caspar T, Somerville C, Preiss J.** 1988. Isolation and characterization of a starchless mutant of *Arabidopsis thaliana* (L.) Heynh lacking ADPglucose pyrophosphorylase activity. *Plant Physiology* **86**, 1131–1135.
- Luo T, Fan T, Liu Y, Rothbart M, Yu J, Zhou S, Grimm B, Luo M.** 2012. Thioredoxin redox regulates ATPase activity of magnesium chelatase CHL1 subunit and modulates redox-mediated signaling in tetrapyrrole biosynthesis and homeostasis of reactive oxygen species in pea plants. *Plant Physiology* **159**, 118–130.
- Meyer Y, Belin C, Delorme-Hinoux V, Reichheld JP, Riondet C.** 2012. Thioredoxin and glutaredoxin systems in plants: molecular mechanisms, crosstalks, and functional significance. *Antioxidants and Redox Signaling* **17**, 1124–1160.
- Michalska J, Zauber H, Buchanan BB, Cejudo FJ, Geigenberger P.** 2009. NTRC links built-in thioredoxin to light and sucrose in regulating starch synthesis in chloroplasts and amyloplasts. *Proceedings of the National Academy of Sciences, USA* **106**, 9908–9913.
- Michelet L, Zaffagnini M, Morisse S, et al.** 2013. Redox regulation of the Calvin–Benson cycle: something old, something new. *Frontiers in Plant Science* **4**, 470.
- Montrichard F, Alkhalfioui F, Yano H, Vensel WH, Hurkman WJ, Buchanan BB.** 2009. Thioredoxin targets in plants: the first 30 years. *Journal of Proteomics* **72**, 452–474.
- Moon JC, Jang HH, Chae HB, et al.** 2006. The C-type *Arabidopsis* thioredoxin reductase ANTR-C acts as an electron donor to 2-Cys peroxiredoxins in chloroplasts. *Biochemical and Biophysical Research Communications* **348**, 478–484.
- Motohashi K, Hisabori T.** 2006. HCF164 receives reducing equivalents from stromal thioredoxin across the thylakoid membrane and mediates reduction of target proteins in the thylakoid lumen. *Journal of Biological Chemistry* **281**, 35039–35047.
- Okegawa Y, Motohashi K.** 2015. Chloroplastic thioredoxin *m* functions as major regulator of Calvin cycle enzymes during photosynthesis *in vivo*. *The Plant Journal* doi: 10.1111/tpj.13049.
- Pérez-Ruiz JM, Guinea M, Puerto-Galán L, Cejudo FJ.** 2014. NADPH thioredoxin reductase C is involved in redox regulation of the Mg-chelatase I subunit in *Arabidopsis thaliana* chloroplasts. *Molecular Plant* **7**, 1252–1255.
- Pérez-Ruiz JM, Spínola MC, Kirchsteiger K, Moreno J, Sahrawy M, Cejudo FJ.** 2006. Rice NTRC is a high-efficiency redox system for chloroplast protection against oxidative damage. *The Plant Cell* **18**, 2356–2368.
- Porra RJ, Thompson WA, Kriedemann PE.** 1989. Determination of accurate extinction coefficients and simultaneous equations for assaying chlorophylls *a* and *b* extracted with four different solvents: verification of the concentration of chlorophyll standards by atomic absorption spectroscopy. *Biochimica et Biophysica Acta – Bioenergetics* **975**, 384–394.
- Puerto-Galán L, Pérez-Ruiz JM, Ferrández J, Cano B, Naranjo B, Nájera VA, González M, Lindahl AM, Cejudo FJ.** 2013. Overoxidation of chloroplast 2-Cys peroxiredoxins: balancing toxic and signaling activities of hydrogen peroxide. *Frontiers in Plant Science* **4**, 310.
- Pulido P, Spínola MC, Kirchsteiger K, Guinea M, Pascual MB, Sahrawy M, Sandalio LM, Dietz K-J, González M, Cejudo FJ.** 2010. Functional analysis of the pathways for 2-Cys peroxiredoxin reduction in *Arabidopsis thaliana* chloroplasts. *Journal of Experimental Botany* **61**, 4043–4054.
- Richter AS, Peter E, Rothbart M, Schlicke H, Toivola J, Rintamäki E, Grimm B.** 2013. Posttranslational influence of NADPH-dependent thioredoxin reductase C on enzymes in tetrapyrrole synthesis. *Plant Physiology* **162**, 63–73.
- Rojas-González JA, Soto-Suárez M, García-Díaz Á, Romero-Puertas MC, Sandalio LM, Mérida Á, Thormählen I, Geigenberger P, Serrato AJ, Sahrawy M.** 2015. Disruption of both chloroplastic and cytosolic FBPase genes results in a dwarf phenotype and important starch and metabolite changes in *Arabidopsis thaliana*. *Journal of Experimental Botany* **66**, 2673–2689.
- Ruban AV, Johnson MP, Duffy CDP.** 2012. The photoprotective molecular switch in the photosystem II antenna. *Biochimica et Biophysica Acta* **1817**, 167–181.
- Sanz-Barrio R, Corral-Martinez P, Ancin M, Segui-Simarro JM, Farran I.** 2013. Overexpression of plastidial thioredoxin *f* leads to enhanced starch accumulation in tobacco leaves. *Plant Biotechnology Journal* **11**, 618–627.
- Schröter Y, Steiner S, Matthäi K, Pfannschmidt T.** 2010. Analysis of oligomeric protein complexes in the chloroplast sub-proteome of nucleic acid-binding proteins from mustard reveals potential redox regulators of plastid gene expression. *Proteomics* **10**, 2191–2204.
- Serrato A, Pérez-Ruiz JM, Spínola MC, Cejudo FJ.** 2004. A novel NADPH thioredoxin reductase, localized in the chloroplast, which deficiency causes hypersensitivity to abiotic stress in *Arabidopsis thaliana*. *Journal of Biological Chemistry* **279**, 43821–43827.

- Serrato AJ, Yubero-Serrano EM, Sandalio LM, Muñoz-Blanco J, Chueca A, Caballero JL, Sahrawy M.** 2009. cpFBPase1, a novel redox-independent chloroplastic isoform of fructose-1,6-bisphosphatase. *Plant, Cell and Environment* **32**, 811–827.
- Spinola MC, Pérez-Ruiz JM, Pulido P, Kirchsteiger K, Guinea M, Gonzalez M, Cejudo FJ.** 2008. NTRC: new ways of using NADPH in the chloroplast. *Physiologia Plantarum* **133**, 516–524.
- Steiner S, Schröter Y, Pfalz J, Pfannschmidt T.** 2011. Identification of essential subunits in the plastid-encoded RNA polymerase complex reveals building blocks for proper plastid development. *Plant Physiology* **157**, 1043–1055.
- Szabó I, Bergantino E, Giacometti GM.** 2005. Light and oxygenic photosynthesis: energy dissipation as a protection mechanism against photo-oxidation. *EMBO Reports* **6**, 629–634.
- Thormählen I, Meitzel T, Groysman J, Öchsner AB, von Roepenack-Lahaye E, Naranjo B, Cejudo FJ, Geigenberger P.** 2015. Thioredoxin *f1* and NADPH-dependent thioredoxin reductase C have overlapping functions in regulating photosynthetic metabolism and plant growth in response to varying light conditions. *Plant Physiology* **169**, 1766–1786.
- Thormählen I, Ruber J, von Roepenack-Lahaye E, Ehrlich SM, Massot V, Hümmel C, Tezycka J, Issakidis-Bourguet E, Geigenberger P.** 2013. Inactivation of thioredoxin *f1* leads to decreased light activation of ADP-glucose pyrophosphorylase and altered diurnal starch turnover in leaves of *Arabidopsis* plants. *Plant, Cell and Environment* **36**, 16–29.
- Wang P, Liu J, Liu B, et al.** 2013. Evidence for a role of chloroplastic m-type thioredoxins in the biogenesis of photosystem II in *Arabidopsis*. *Plant Physiology* **163**, 1710–1728.
- Wimmelbacher M, Börnke F.** 2014. Redox activity of thioredoxin *z* and fructokinase-like protein 1 is dispensable for autotrophic growth of *Arabidopsis thaliana*. *Journal of Experimental Botany* **65**, 2405–2413.
- Wolosiuk RA, Buchanan BB.** 1976. Studies on the regulation of chloroplast NADP-linked glyceraldehyde-3-phosphate dehydrogenase. *Journal of Biological Chemistry* **251**, 6456–6461.
- Wolosiuk RA, Crawford NA, Yee BC, Buchanan BB.** 1979. Isolation of three thioredoxins from spinach leaves. *Journal of Biological Chemistry* **254**, 1627–1632.
- Yoshida K, Hara S, Hisabori T.** 2015. Thioredoxin selectivity for thiol-based redox regulation of target proteins in chloroplasts. *Journal of Biological Chemistry* **290**, 14278–14288.
- Yoshida K, Matsuoka Y, Hara S, Konno H, Hisabori T.** 2014. Distinct redox behaviors of chloroplast thiol enzymes and their relationships with photosynthetic electron transport in *Arabidopsis thaliana*. *Plant and Cell Physiology* **55**, 1415–1425.
- Zhang N, Portis AR.** 1999. Mechanism of light regulation of Rubisco: a specific role for the larger Rubisco activase isoform involving reductive activation by thioredoxin-*f*. *Proceedings of the National Academy of Sciences, USA* **96**, 9438–9443.